

Identifying Linear Relational Concepts in Large Language Models

David Chanin, Anthony Hunter and Oana-Maria Camburu

Department of Computer Science
University College London
London, UK

Abstract

Transformer language models (LMs) have been shown to represent concepts as directions in the latent space of hidden activations. However, for any given human-interpretable concept, how can we find its direction in the latent space? We present a technique called *linear relational concepts* (LRC) for finding concept directions corresponding to human-interpretable concepts at a given hidden layer in a transformer LM by first modeling the relation between subject and object as a linear relational embedding (LRE) (Hernandez et al., 2023b). While the LRE work was mainly presented as an exercise in understanding model representations, we find that inverting the LRE while using earlier object layers results in a powerful technique to find concept directions that both work well as a classifier and causally influence model outputs.

1 Introduction

How do large language models (LLMs) represent concepts, and how can we identify those concepts in hidden activations? If we can identify human-interpretable concepts in model activations, we can analyze how concepts are created and change during inference. Identifying concept representations inside of models opens up the possibility of visualizing the computation process of models as sentences are processed, and can help to understand incorrect or undesirable responses from the model. Moreover, future work examining how concept directions link together inside the model may benefit from a robust method to find those concept directions as a first step.

An intuitive approach when trying to locate a human-interpretable concept, like the concept of a city being in France, is to collect examples of sentences with cities that are in France and cities that are not, and train a probing classifier (Ettinger et al., 2016; Finlayson et al., 2021) on hidden layers of the model, typically a simple linear classi-

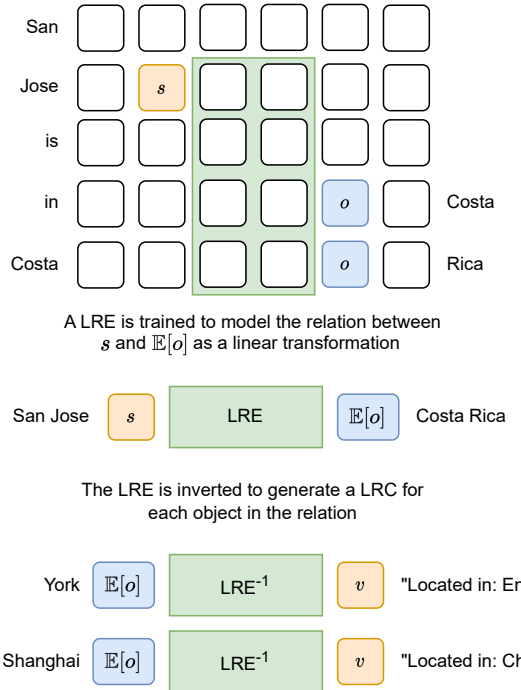


Figure 1: We first model the relation between the subject s and object o as an affine linear transformation called a linear relation embedding (LRE). We find that inverting the LRE to output subject activations as a function of object from the relation results in concept directions that serve both as classifiers and causally impact model outputs. In the above figure, we train an LRE from the statement “San Jose is in Costa Rica”, and then invert that LRE to create linear relational concepts (LRCs) representing “located in England” and “located in China” by providing representations of “York” and “Shanghai”, respectively.

fier. However, the learned classifier may be picking up features correlated with the concept being probed while overlooking the feature direction that causally influences model output (Hernandez et al., 2023b).

Furthermore, the hidden layer in modern transformer models has high dimensionality: even older models such as GPT2-xl have 1600 dimensions in the hidden layer (Radford et al., 2019), and mod-

ern language models such as Llama2-7b have over 4000 dimensions for the smallest model (7B) (Touvron et al., 2023). As a result, naively training a probing classifier may require a high number of training samples.

Our technique builds on work by Hernandez et al. (2023b), which models the relation between a subject s and object o as an affine linear transformation, called a linear relational embedding (LRE). While the LRE work is mainly an investigation into how models represent relational knowledge, we find that inverting LREs results in concept directions that achieve surprisingly strong performance as linear classifiers while also causally impacting model outputs, outperforming standard probing classifiers such as support vector machines (SVMs). We refer to the concept directions that our method creates as linear relational concepts (LRCs). LRCs represent concepts as directions in a latent space, while also functioning as linear classifiers.

We generate LRCs using inverted LREs, as illustrated in Figure 1. We first generate an LRE for a relation, mapping subject activations in that relation to their corresponding object activations. Then, we perform a low-rank inverse of the LRE, mapping from object activations to subject activations. We find that this low-rank inverse of the LRE results in LRCs that beat traditional probing classifiers in both classification accuracy and causality, where causality is defined as being able to control the output of the model. For instance, we might force the model to output that “London is located in France” by subtracting the “Located in England” direction from the activation of “London” and adding the “Located in France” direction.

In addition, LRCs improve on the original LRE work by allowing us to map subject activations to object activations before the final layer of the model, and to use all object token activations rather than only using the first object token. This improves classification accuracy for both single-token and multi-token objects compared with the original LRE work, which must always map to the final layer of the model and use only the first object token.

In summary, in this paper, we investigate the problem of locating human-interpretable concepts within LLM activations. We present a technique for finding human-interpretable concept directions, called LRC, in the hidden layer of auto-regressive LLMs such as GPT (Radford et al., 2019) and

Llama (Touvron et al., 2023). We evaluate our technique using the LRE relations dataset (Hernandez et al., 2023b), and evaluate our approach in both one-vs-all classification accuracy, and causality (the ability of concepts to modify model output). Our technique achieves high scores for both classification accuracy and causality across all the four concept types in the LRE relations dataset.

Our contributions include the following: (1) Extending LREs to handle multi-token objects, (2) Using non-terminal model layers for the object activation, and (3) Using inverted LREs as an intermediate step to find concept directions in subject activations.

2 Background

Previous work on transformer models has shown that features are stored as directions within the latent space of the model’s hidden activations, known as the linear representation hypothesis (Elhage et al., 2022). We subscribe to this theory, and thus look for concepts as direction vectors in the model activations.

Further work has shown that mid-level multi-layer perceptron (MLP) layers in transformer LLMs act as key-value stores of information (Geva et al., 2021). These MLP layers enhance the final token of the subject of the sentence (e.g. the token “lin” in “Berlin is located in the country of”) with this information in factual relations (Geva et al., 2023; Meng et al., 2022).

2.1 Linear Relational Embeddings

Linear relational embeddings (LREs) were first presented by Paccanaro and Hinton (2001) as a way to encode relational concepts as a linear transformation. Hernandez et al. (2023b) showed that for some relations, transformer LMs appear to encode relational knowledge using LREs. They model the processing performed by a transformer LLM mapping from a subject s to an object o within a textual context c as a linear transformation $o = F(s, c) = Ws + b$, where $W \in \mathbb{R}^{H \times H}$, $b \in \mathbb{R}^H$. This function F is estimated by a first-order Taylor approximation around s , while W and b are calculated as the mean Jacobian and bias of n samples s_i, c_i from relation r , respectively:

$$W = \mathbb{E}_{(s_i, c_i)} \left[\frac{\partial F}{\partial s} \Big|_{(s_i, c_i)} \right]$$

$$b = \mathbb{E}_{(s_i, c_i)} \left[F(s, c) - \frac{\partial F}{\partial s} s \Big|_{(s_i, c_i)} \right]$$

A hyperparameter β is used to increase the slope of the LRE and can be configured to improve the performance of the LRE in the case that the Jacobian underestimates the steepness of W , resulting in the following equation for a LRE R :

$$R(s) = \beta W s + b$$

LREs are evaluated on *faithfulness* and *causality*. The faithfulness metric checks if the LRE output matches what the model outputs for the first predicted token when presented with a new subject. For instance, if an LRE trained on the relation “city in country” predicts the token “France” as the most likely output given the subject activation of “Paris”, the LRE is said to be faithful. However, this limits the LRE to modeling only a single token of object o at the final layer of the model. As a result, LREs cannot distinguish between words that start with the same token. For example, “Bill Gates” and “Bill of Rights” both begin with the token “Bill”, and thus cannot be distinguished by an LRE when evaluated for faithfulness.

To evaluate the causality of the LRE, the LRE is inverted using a low-rank pseudo-inverse of the weight matrix, indicated W^\dagger . [Hernandez et al. \(2023b\)](#) find that using a low-rank pseudo-inverse results in better performance than using a full-rank inverse. This inversion makes it possible to calculate a delta Δs that could be added to the subject s to cause the model to change its output from the original object o to a new object o' . Causality is evaluated based on whether the model’s probability of outputting o' is greater than the probability of outputting o after the edit:

$$\Delta s = W^\dagger(o - o')$$

We build our method from this technique of inverting the LRE weight matrix to target the subject activations rather than object activations.

3 Method

Our method finds an LRC, represented as a concept direction vector, v , for a given human-interpretable

concept in the hidden activations of a transformer LLM model at a layer l . Since we are interested in concepts as directions in the hidden activation space of the model, we ignore a bias term and focus on learning only a single unit-length vector to represent the LRC.

Formally, we consider an auto-regressive model $G : \mathcal{X} \rightarrow \mathcal{Y}$ with vocabulary V that maps a sequence of tokens $x = [x_1, \dots, x_T] \in \mathcal{X}, x_i \in V$ to a probability distribution $y \in \mathcal{Y} \subset \mathbb{R}^{|V|}$ that predicts the next token of x . Internally, G has a hidden state size H , and has L layers. The hidden activations of layer l of G at token i is represented by $h_i^{(l)} \in \mathbb{R}^H$.

We follow the example of [Meng et al. \(2022\)](#) and [Hernandez et al. \(2023b\)](#), and consider statements of the form (s, r, o) consisting of a subject s , relation r , and object o . For instance, the statement “Paris is located in the country of France” would have subject “Paris”, object “France”, and relation “located in country”. Our definition of a concept corresponds to a relation and object pair (r, o) , which operates on the activations of the subject s . So in our case, we would learn an LRC for the concept “located in country: France”, and would expect the LRC to have high similarity with the subject activations of “Paris”, but not the activations of “Berlin” or “Tokyo”.

We build on the LRE work by [Hernandez et al. \(2023b\)](#), however we make the following changes to the original LRE method. We use the mean of all object token activations rather than just the first object token activation to better handle multi-token objects. We also relax the requirement that only the final layer can be used for object activations, since we find that classification performance improves substantially by using non-final layers for the object. Finally, we restrict training samples for the LRE to only contain examples where the model answers the prompt correctly. If the model does not know the answer to a prompt, we assume that the relevant conceptual knowledge we hope to capture in the LRC is not present, and that the sample will likely be noise.

For a relation r , we have a set of possible objects O that can be the object for the relation, and each object o has a corresponding set of subjects S_o , where each subject $s_o \in S_o$ corresponds to object o . We first assemble prompts that elicit each object $o \in O$ for the relation r . For example, for the relation “Located in country”, prompts fol-

Prompt (s, r)	Object (o)
Paris is located in the country of	France
Berlin is located in the country of	Germany
Suzhou is located in the country of	China
Tokyo is located in the country of	Japan
Lyon is located in the country of	France
Manaus is located in the country of	Brazil

Table 1: Sample prompts and corresponding object for the relation “Located in country”.

low the template “⟨SUBJECT⟩ is located in the country of”. Some examples of prompts and their corresponding objects are shown in Table 1.

For a relation for which we wish to build a set of LRCs, we assume a set of prompts containing subject s and relation r , and we expect the model to predict o . We use hidden states from the final token index i of subject s . For the subject “Berlin”, this tokenizes to “Ber” and “lin” when using the GPT tokenizer, so i corresponds to the token “lin” as this is the final subject token.

We first select n prompts from r , balancing the prompts to have as even a distribution of prompts across O . Following Hernandez et al. (2023b), we train a LRE $R(s)$ consisting of a weight matrix W and bias b using these n prompts, however we calculate the weight matrix W using the Jacobian of the mean of all object tokens, not only the first object token. This change means we model $F(s, c)$ as follows:

$$\mathbb{E}[o] = F(s, c) = Ws + b$$

This is the same as the original LRE formulation if the object consists of a single token.

We also ignore the β scaling factor from the original LRE definition. LRCs are normalized to have unit length, and this normalization will remove any scaling applied to the LRE. Our definition of an LRE, denoted $R(s)$, is thus simplified as follows:

$$R(s) = Ws + b$$

We then invert $R(s)$ to get $R^{-1}(o)$, which maps object activations to subject activations. However, following Hernandez et al. (2023b), we use a low-rank pseudo-inverse, denoted R^\dagger rather than the full matrix inverse R^{-1} :

$$R^\dagger(o) = W^\dagger(o - b)$$

To calculate the LRC v_o for o , we take the mean of all samples of $R^\dagger(o)$ for each prompt (s, r, o) in our training set:

$$\hat{v}_o = \mathbb{E}[W^\dagger(h_o - b)]$$

Finally, we normalize the LRC direction to have unit length:

$$v_o = \frac{\hat{v}_o}{\|\hat{v}_o\|}$$

This normalization is done since we are interested in concepts as directions only.

4 Results

We evaluate our method using the relations dataset from Hernandez et al. (2023b), which contains prompts for 47 relation types each with a variety of subject and object pairs, containing over 10,000 instances in total. The dataset divides relation types into four categories: factual knowledge, linguistic knowledge, commonsense knowledge, and implicit bias. A subset of data from a sample relation in the dataset is shown in Table 2. Statistics about the number of relations and samples per category are shown in Table 3.

We evaluate our performance using two metrics. The first, classification accuracy, treats each relation as a one-vs-all classification problem, where the LRC with the highest dot-product similarity to the test subject activation is considered to be the predicted object \hat{y} . Since all LRCs are normalized to have unit length, this is equivalent to picking the LRC with the highest cosine similarity:

$$\hat{y} = \operatorname{argmax}_{o \in O} v_o \cdot a$$

To evaluate causality, we randomly pick a different object o_c for prompts corresponding to each subject in a relation and edit the subject token activations to predict the new counterfactual object o' instead of the original object o . We subtract the original LRC from the final subject token activations at all layers, and add in the new LRC. For instance, we may attempt to edit the prompt “Paris is located in the country of” to predict “Germany” instead of “France” by subtracting the “located in country: France” concept and adding the “located in country: Germany” concept.

The direction vector in our LRCs are all normalized to unit length, so we scale the LRCs by a

hyperparameter $\beta \in [0, 1]$ multiplied by the magnitude of the subject activation at each layer before adding or subtracting them. The causal edit at a layer l is thus calculated as below:

$$\Delta s^{(l)} = \beta \|h_i^{(l)}\| (v_{o'} - v_o)$$

The causality intervention is considered successful if the probability of predicting the counterfactual object o' after the edit is higher than the probability of predicting the original object o . For multi-token predictions, we use the minimum probability across all predicted tokens rather than multiplying token probabilities to avoid penalizing objects that require more tokens to represent. Experimentally, $\beta = 0.05$ works well for GPT-J and $\beta = 0.075$ works well for Llama2-7b.

We perform a multi-layer edit in our causality evaluation rather than a single-layer edit as in Hernandez et al. (2023b), since we feel that single-layer causality unfairly penalizes learning concepts in later layers of the model. Since only one layer is edited in single-layer causality, the model will still attend to the unedited subject activations for earlier layers, which penalizes using a later layer to find concept directions. Instead, we perform the same edit at all layers of the subject, so there is no inherent penalty to using a later layer to learn the LRC, and the model does not attend to any unedited subject activations. In addition, editing all layers avoids the need to search for a single optimal layer to perform each edit.

We evaluate against both Llama2-7b (Touvron et al., 2023) and GPT-J (Wang and Komatsuzaki, 2021). We focus on Llama2-7b for our analysis as it is a more advanced model than GPT-J, but we include full results for GPT-J in Appendix A. GPT-J is included as this model was used in the original LRE paper.

For each relation, we split the dataset into a 50%/50% train/test split by relation and object, ensuring at least one training example is present per object in the relation. We prepend four other examples from the same relation to each training example to act as few-shot learning examples. However, during causality and classification benchmarks, we use only zero-shot prompts from the dataset, following the procedure in the original LRE paper. An example few-shot prompt is shown in Figure 2. This process is repeated five times with different random seeds for train/test splits, and results are averaged across the results from each seed. The

relation: city in country		
FS	{ } is part of { } is in the country of	
ZS	{ } is part of the country of { } is located in the country of	
subject	object	
New York City	United States	
Rio de Janeiro	Brazil	
Kuala Lumpur	Malaysia	
Las Vegas	United States	
Johannesburg	South Africa	
Panama City	Panama	
Saint Petersburg	Russia	

Table 2: Sample relation data for the “city in country” relation from the dataset, showing zero-shot (ZS) prompt templates, few-shot (FS) prompt templates, and several subject / object pairs. In each prompt template, { } is replaced with a subject.

Category	Relations	Samples
Commonsense	7	337
Bias	7	212
Factual	21	9462
Linguistic	4	660

Table 3: Statistics for the number of relations and samples of each category in the dataset after filtering out one-to-one relations.

Tokens	Llama2-7b samples	GPT-J samples
1	2393	2108
2	451	39
3	371	2
4	107	6
5+	4	0

Table 4: Statistics for the average number of tokens in objects for the test set for Llama2-7b and GPT-J after filtering out one-to-one relations and samples which the model answers incorrectly. The majority of samples are single-token, but Llama2-7b still answers correctly a large number of multi-token object samples. GPT-J performs worse than Llama2-7b especially on multi-token object samples, barely answering any correctly.

The superlative form of bad is worst
 The superlative form of big is biggest
 The superlative form of brave is bravest
 The superlative form of bright is brightest
 The superlative form of angry is

Figure 2: Sample few-shot (FS) prompt for the relation “adjective superlative”, subject “angry”, and object “angriest” from the dataset. FS prompts are used for training, while testing consists only of zero-shot (ZS) prompts.

shaded area in plots corresponds to this standard deviation.

For some relations, there is a one-to-one mapping between subject and object, so it is impossible to create a test split with unseen subject/object pairs to evaluate. An example of a relation of this type is “capital city of country”. Each country has one capital city, and each capital city is the capital of only one country. Since our definition of a concept includes a unique r and o pair, we are unable to evaluate these relations and exclude them from the evaluation. We furthermore exclude any relations with less than five test samples after filtering as having so few test samples makes it hard to evaluate performance robustly.

When training LRCs via inverted LREs using our method, we use five training samples per LRE, and use rank 192 for the low-rank pseudo-inverse, unless specified otherwise. All calculations are performed using 16-bit quantization. Unless otherwise specified, all evaluations are performed with subject layer 17 and object layer 21 for Llama2-7b, and subject layer 14 and object layer 20 for GPT-J.

For objects that tokenize to multiple tokens, we evaluate against the full multi-token output. All prompts for both train and test datasets are pre-filtered to exclude any prompts where the model gives an incorrect answer, since if the model does not get the correct answer it is unclear that the concept being classified will be elicited in the hidden activations at all.

4.1 Comparisons

We compare our method against training a standard linear support vector machine (SVM) classifier on the hidden activation data, as well as estimating a concept direction by simply averaging together the hidden activations for a given object.

We also compare our method to a LRC trained using the final layer for the object token, as in the

Llama2-7b		
Method	Accuracy	Causality
LRC (mean, l_{21})	0.81 ± 0.01	0.78 ± 0.02
LRC (ft, l_{final})	0.74 ± 0.02	0.78 ± 0.02
SVM	0.73 ± 0.02	0.69 ± 0.01
Input averaging	0.70 ± 0.01	0.55 ± 0.03

GPT-J		
Method	Accuracy	Causality
LRC (mean, l_{20})	0.81 ± 0.02	0.84 ± 0.01
LRC (ft, l_{final})	0.78 ± 0.02	0.86 ± 0.01
SVM	0.75 ± 0.02	0.76 ± 0.01
Input averaging	0.73 ± 0.03	0.56 ± 0.02

Table 5: Classification accuracy and causality results on the relations dataset for Llama2-7b and GPT-J. LRC is our method. “mean” refers to using the mean of all object tokens to calculate the LRE, while “ft” refers to using only the first token of the object to calculate a LRE. LRC (ft, l_{final}) is included as an ablation to best estimate the results of inverting the original LRE technique at the final layer. Results include mean and standard deviation after five random seeds.

original LRE paper where the final layer is always used for objects.

4.2 Classification accuracy and causality

For both classification accuracy and causality, we calculate a score per relation, and then average the scores across relations. We do this because some relations have more test samples than other relations, which would otherwise bias the results towards to reflect whichever relation has the most test samples and not give a good reflection of performance across the full range of relation types in the relations dataset.

We measure classification accuracy and causality on the relations dataset for our method, our method ablating the alignment loss, using a pure SVM, and using activation averaging. Results are shown in Table 5.

Our method performs the best on both classification accuracy and causality. Classification accuracy improves by a large margin simply by using layer 28 instead of the final Llama2-7b layer 31, showing the importance of allowing the LRE to use a non-terminal layer.

4.3 Multi-token vs single-token objects

We also compare the performance of LRCs on single-token and multi-token objects. One of the main limitations of the original LRE work is not being able to handle multi-token objects, so we expect the improvement of our method over traditional LREs to be most stark for multi-token objects.

To investigate the impact of the final object layer on single-token and multi-token performance, we evaluate our method on each layer from layer 18 to the final layer 31 for Llama2-7b keeping layer 17 as the subject layer. We only use Llama2-7b for this comparison since GPT-J has very few multi-token prompts from the dataset that it can answer correctly. Multi-token classification accuracy and causality by object layer is shown in Figure 3. Single-token classification accuracy and causality by object layer is shown in Figure 4.

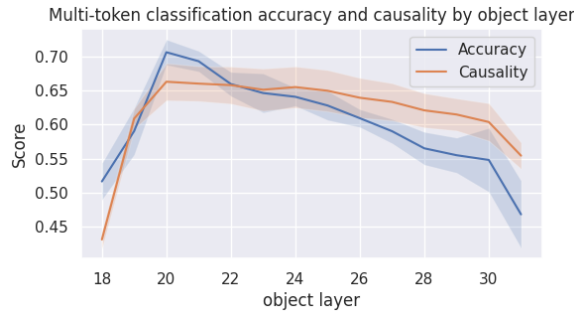


Figure 3: Classification accuracy and causality by object layer for multi-token objects on Llama2-7b. Shaded area indicates standard deviation after five seeds.

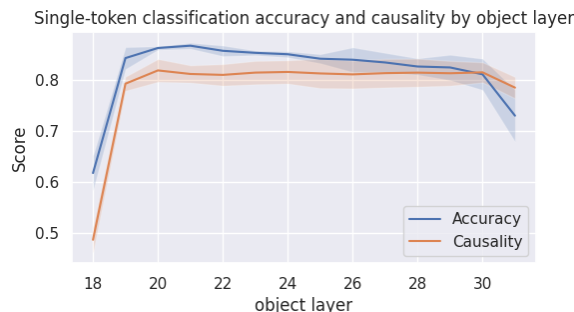


Figure 4: Classification accuracy and causality by object layer for single-token objects on Llama2-7b. Shaded area indicates standard deviation after five seeds.

Both single-token and multi-token performance improves by using earlier object layers, but the difference is especially pronounced for multi-token objects.

4.4 Impact of the rank of the LRE inverse

One of the surprising results from Hernandez et al. (2023b) is that using a low-rank inverse of the LRE results in better performance than using a full-rank inverse. We investigate this relationship between the rank of the LRE inverse and performance on the relations dataset for the LRC method as well. Classification accuracy and causality results are shown in Figure 5.

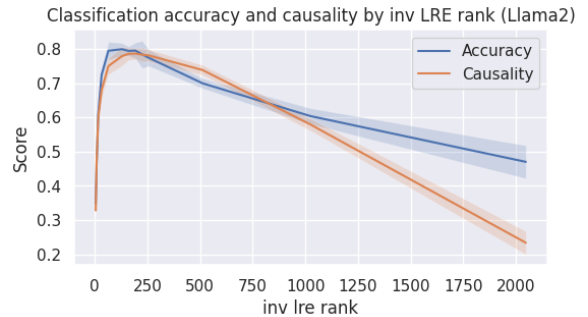


Figure 5: Classification accuracy and causality on the relations dataset by LRE inversion rank on Llama2-7b. Shaded area indicates standard deviation after five seeds.

Using a low-rank LRE inverse improves performance dramatically, and with performance peaking around rank 200 for Llama2-7b. Llama2-7b has a 4096 dimension hidden space, so a full-rank inverse would have rank 4096, meaning a rank 200 inverse is discarding over 90% of the LRE weight matrix. We suspect that the generalization power of using an inverted LRE to find concept directions comes from this low-rank inverse, where the most important common components of the relation are captured in a small portion of the LRE weight matrix.

4.5 Choosing samples to train the LRE

We follow the example of Hernandez et al. (2023b) and use a small subset of the available training samples to train the LRE. For our method, we use the LRE only as an intermediate step in deriving a LRC, which makes it possible to train a LRE optimized to perform best on the specific relation and object (r, o) we are interested in training a LRC for. A natural instinct is to only choose samples for the LRE which contain only the object in question. For instance, to train a LRC for “Located in country: France”, it would seem natural to only use training samples consisting of cities in France to train the LRE, rather than cities in other countries.

We investigate this in the simplest case of us-

LRE train sample	Accuracy	Causality
Same object	0.31 ± 0.04	0.31 ± 0.02
Different object	0.69 ± 0.01	0.70 ± 0.02

Table 6: Results for training a LRC derived from a LRE trained with a single training sample for the relations dataset, where that sample either represents the same object as the LRC (Same object) or a different object in the same relation (Different object). Unintuitively, when the sample the LRE is trained on is the same object as the LRC, the LRC performs extremely poorly. These results are from Llama2-7b.

ing only a single training sample to train the LRE, since for many objects in the relations dataset only a single training sample is available. We compare training the LRE using and LRC using a sample which represents the same object, as well as training a LRE with a sample which is from another object in the same relation, but not the object the LRC will represent. The results of this experiment are shown in Table 6.

Unintuitively, training the LRE using a sample with the same object as the LRC results in dramatically worse performance. We do not yet understand why this is, but suspect that choosing samples from different objects may have a regularizing effect on the resulting LRC. Using the same object to train a LRE and also extract a LRC is equivalent to estimating the concept direction on the subject as the derivative relative to the object, but it is possible that this results in directions which may be unrealistic in practice. More investigation will be necessary to understand this phenomena in-depth, but for our purposes we find that it is essential that the training samples for the LRE contain different objects from the same relation, not only the same object as the LRC.

4.6 Subject layer causality vs accuracy

While we try to address the issue that using a later subject layer for LRC training results in fewer opportunities to causally intervene in the model processing by evaluating causality by performing a multi-layer edit, we still find a trade-off between causality and classification accuracy depending on the subject layer of LRC. Using an earlier layer allows us to find the maximally causal intervention to change model outputs, but means that classification accuracy suffers since the MLP layers of the model have not yet had a chance to fully enhance

the subject token with relevant information about the subject. Figure 6 shows classification accuracy and causality results on the relations dataset for training the LRC using subject layer 10 through 21, with object layer 22 on Llama2-7b.

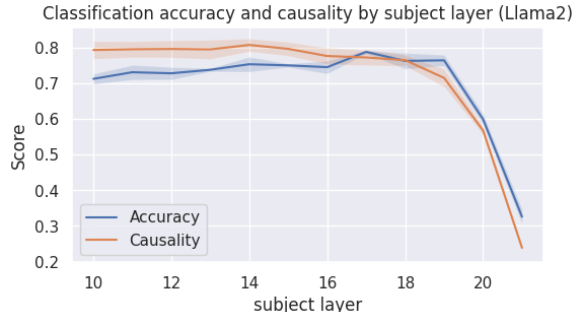


Figure 6: Classification accuracy and causality on the relations dataset by subject layer on Llama2-7b with object layer 22. Shaded area indicates standard deviation after five seeds.

We see causality being highest with earlier layers, while classification accuracy appears to roughly increase up to layer 19, after which performance rapidly declines. We suspect this trade-off is a limitation of learning a LRC using a single pair of subject and object layers, and that it may be possible to combine LRCs learned at different layers to find a direction which achieves both peak classification accuracy and causality.

5 Related work

Previous work on understanding how deep neural networks represent concepts focuses on understanding individual neurons (Bills et al., 2023; Yosinski et al., 2015). However, individual neurons have been found to activate in response to multiple different concepts, making a clean, human-interpretable understanding of each neuron difficult (Goh et al., 2021). Indeed, transformers can represent more concepts than they have neurons in their hidden layers (Elhage et al., 2022).

A great source of inspiration for this work has been work on knowledge editing in language models, specifically ROME (Meng et al., 2022) and REMEDI (Hernandez et al., 2023a). In ROME, factual knowledge is shown to reside in the mid-layer MLP of language models, and this knowledge can be edited by updating an arbitrary mid-layer MLP to insert any fact desired. ROME finds the appropriate update by means of counterfactual backpropagation, similar to our work. Indeed, ROME was

as a main source of inspiration and a starting point for our work.

In REMEDI, model outputs are edited by adding a vector to the subject of a sentence during the forward inference pass. This is similar to our work in that this vector being added to the hidden activations of a subject can be said to contain the concept that is desired to be elicited. However, the goal of REMEDI is to edit model outputs rather than identifying concept direction vectors and building a classifier like in our work.

We also take inspiration from work on probing classifiers (Belinkov, 2022; Ettinger et al., 2016). Probing classifiers are simple, typically linear, classifiers which operate on hidden activations inside of neural networks to determine if the activations. TCAV (Kim et al., 2018) can be said to be a probing classifier for vision models, where a classifier is learned at multiple layers in the model. Most similar to our work, (Li et al., 2021) build a probing classifier to identify states in a world model for textual games from language model hidden activations, and show that the hidden activations of neural networks do encode a basic world model. However, this work focuses on encoder-decoder models, and does not attempt to classify arbitrary human-interpretable concepts outside of the text game context. This work also takes the approach of directly training a linear classifier for a given concept known to be present in the encoder activations rather than directly trying to find a concept direction as in our work.

The most similar to this paper is work on Linear Relational Embedding concepts in LLMs (Hernandez et al., 2023b), which is the source for our evaluation dataset and serves as the first step in our method. This work also attempts to estimate relational concepts, and does so by learning a linear affine transformation from the subject token activation at layer l to the first output token of the object at the final layer of the model. However, as LRE concepts only map to the first object token, they are not suited to multi-token objects. For instance, a LRE cannot distinguish between “Bill Gates” and “Bill Clinton” as they both begin with the same token. In addition, the original LRE work is presented as a means of understanding how LLMs may encode information rather than attempting to build a classifier or find concept directions as in our work.

6 Conclusion

Identifying and classifying a broad set of human-interpretable concepts in language model activations is a vital step towards understanding and debugging how language models operate. In this work, we have shown a technique for identifying and classifying concepts in model hidden activations using inverted LREs. We show that our technique is both a better classifier and learns directions with higher causality than standard linear classifiers like SVM.

While our technique performs well, there is still a large amount of variance in performance depending on the training samples chosen. We expect further improvements can be achieved by determining which LRE training samples will result in the best performance for each LRC. In addition, we suspect that it should be possible to combine LRCs learned at multiple layers to find concept directions that achieve even better results to get around the trade-off of causality performing best with earlier subject layer LREs, and classification accuracy performing better with later subject layer LREs.

In the future, we hope concept identification techniques such as this will make it possible to investigate the relations between concepts within model weights, and extract learned knowledge and even world models directly from pretrained language models.

Limitations

Our method requires learning a new LRC for every (r, o) pair, so cannot generalize to new objects without a training sample of that (r, o) . Our evaluation also assumes that each subject maps only to a single object in the same relation, and would need modifications to handle subjects with multiple objects in the same relation, such as a movie that can have multiple genres, but we do not investigate that in this work.

Our method assumes that each human-interpretable concept corresponds to a direction in the hidden space of the model, and we assume that if the model outputs the correct answer to a prompt then the model has a representation of this concept in its activations. However, it is also possible for the model to guess the correct answer without having any underlying representation, which will cause our method to not perform well. For instance, for the prompt “Sam Eastwood’s father is named”, the model will output the correct

answer “Clint Eastwood”. However, did the model have an underlying representation of this fact in its hidden activations, or is it simply guessing the most famous person with the last name “Eastwood”, which is Clint Eastwood? Indeed, GPT-J will output “Clint Eastwood” as the father of almost any made up person with the last name “Eastwood”. Our method would likely perform much better if these cases where the model can guess the correct answer were filtered out, but differentiating between the model guessing and knowing the correct answer is challenging.

Recent work suggests that sometimes the knowledge that maps subjects to objects is not present in MLP layers applied to the subject token, but instead is contained directly in attention values and only is added to the residual stream of the output tokens instead of the subject (Geva et al., 2023). For knowledge of this sort, our method will fail since we assume all knowledge can be found in the subject token residual stream rather than needing to look at the output token.

Finally, our method works only for relational concepts of the form (s, r, o) . Other types of concepts which do not easily fit into this format would require an adaptation or a different technique.

Acknowledgements

Oana-Maria Camburu was supported by a Leverhulme Early Career Fellowship. David Chanin was supported with thanks to EPSRC EP/S021566/1.

References

- Yonatan Belinkov. 2022. Probing classifiers: Promises, shortcomings, and advances. *Computational Linguistics*, 48(1):207–219.
- Steven Bills, Nick Cammarata, Dan Mossing, Henk Tillman, Leo Gao, Gabriel Goh, Ilya Sutskever, Jan Leike, Jeff Wu, and William Saunders. 2023. Language models can explain neurons in language models. URL <https://openaipublic.blob.core.windows.net/neuron-explainer/paper/index.html>. (Date accessed: 14.05. 2023).
- Nelson Elhage, Tristan Hume, Catherine Olsson, Nicholas Schiefer, Tom Henighan, Shauna Kravec, Zac Hatfield-Dodds, Robert Lasenby, Dawn Drain, Carol Chen, et al. 2022. Toy models of superposition. *arXiv preprint arXiv:2209.10652*.
- Allyson Ettinger, Ahmed Elgohary, and Philip Resnik. 2016. Probing for semantic evidence of composition by means of simple classification tasks. In *Proceedings of the 1st workshop on evaluating vector-space representations for nlp*, pages 134–139.
- Matthew Finlayson, Aaron Mueller, Sebastian Gehrmann, Stuart Shieber, Tal Linzen, and Yonatan Belinkov. 2021. Causal analysis of syntactic agreement mechanisms in neural language models. In *Proceedings of the 59th Annual Meeting of the Association for Computational Linguistics and the 11th International Joint Conference on Natural Language Processing (Volume 1: Long Papers)*, pages 1828–1843, Online. Association for Computational Linguistics.
- Mor Geva, Jasmijn Bastings, Katja Filippova, and Amir Globerson. 2023. Dissecting recall of factual associations in auto-regressive language models. *arXiv preprint arXiv:2304.14767*.
- Mor Geva, Roei Schuster, Jonathan Berant, and Omer Levy. 2021. Transformer feed-forward layers are key-value memories. In *Proceedings of the 2021 Conference on Empirical Methods in Natural Language Processing*, pages 5484–5495, Online and Punta Cana, Dominican Republic. Association for Computational Linguistics.
- Gabriel Goh, Nick Cammarata, Chelsea Voss, Shan Carter, Michael Petrov, Ludwig Schubert, Alec Radford, and Chris Olah. 2021. Multimodal neurons in artificial neural networks. *Distill*, 6(3):e30.
- Evan Hernandez, Belinda Z Li, and Jacob Andreas. 2023a. Measuring and manipulating knowledge representations in language models. *arXiv preprint arXiv:2304.00740*.
- Evan Hernandez, Arnab Sen Sharma, Tal Haklay, Kevin Meng, Martin Wattenberg, Jacob Andreas, Yonatan Belinkov, and David Bau. 2023b. Linearity of relation decoding in transformer language models. *arXiv preprint arXiv:2308.09124*.
- Been Kim, Martin Wattenberg, Justin Gilmer, Carrie Cai, James Wexler, Fernanda Viegas, et al. 2018. Interpretability beyond feature attribution: Quantitative testing with concept activation vectors (tcav). In *International conference on machine learning*, pages 2668–2677. PMLR.
- Belinda Z. Li, Maxwell Nye, and Jacob Andreas. 2021. Implicit representations of meaning in neural language models. In *Proceedings of the 59th Annual Meeting of the Association for Computational Linguistics and the 11th International Joint Conference on Natural Language Processing (Volume 1: Long Papers)*, pages 1813–1827, Online. Association for Computational Linguistics.
- Kevin Meng, David Bau, Alex Andonian, and Yonatan Belinkov. 2022. Locating and editing factual associations in gpt. *Advances in Neural Information Processing Systems*, 35:17359–17372.

Alberto Paccanaro and Geoffrey E. Hinton. 2001. Learning distributed representations of concepts using linear relational embedding. *IEEE Transactions on Knowledge and Data Engineering*, 13(2):232–244.

Alec Radford, Jeffrey Wu, Rewon Child, David Luan, Dario Amodei, Ilya Sutskever, et al. 2019. Language models are unsupervised multitask learners. *OpenAI blog*, 1(8):9.

Hugo Touvron, Louis Martin, Kevin Stone, Peter Albert, Amjad Almahairi, Yasmine Babaei, Nikolay Bashlykov, Soumya Batra, Prajjwal Bhargava, Shruti Bhosale, et al. 2023. Llama 2: Open foundation and fine-tuned chat models. *arXiv preprint arXiv:2307.09288*.

Ben Wang and Aran Komatsuzaki. 2021. Gpt-j-6b: A 6 billion parameter autoregressive language model.

Jason Yosinski, Jeff Clune, Anh Nguyen, Thomas Fuchs, and Hod Lipson. 2015. Understanding neural networks through deep visualization. In *Deep Learning Workshop, International Conference on Machine Learning (ICML)*.

A Appendix

A.1 Extended results

Full results broken down by each relation tested is shown in Figure 7 for Llama2-7b, and 8 for GPT-J. These plots compare the results for our method (LRC) against the results for support vector machines (SVM).

Results for the effect of the rank of the LRE weight matrix inverse on performance of the LRC method for GPT-J is shown in Figure 9.

Results illustrating the effect of object layer choice our method for GPT-J is shown in Figure 10, with subject layer 15. We do not break down the effect of this object layer choice by single-token vs multi-token objects since GPT-J answers very few multi-token object prompts correctly.

Results illustrating the effect of the subject layer choice on LRC performance are shown in Figure 11 with object layer 20. As with Llama2-7b, we find a trade-off between causality and classification accuracy, where earlier layers result in better causality performance at the expense of classification accuracy.

A.2 Statistical significance

We calculate statistical significance between our method (LRC) and SVM for classification accuracy and causality. We find that LRCs performance improvement over SVM is statistically significant.

We use a two-proportion Z-test to calculate significance. Since we run five random seeds with

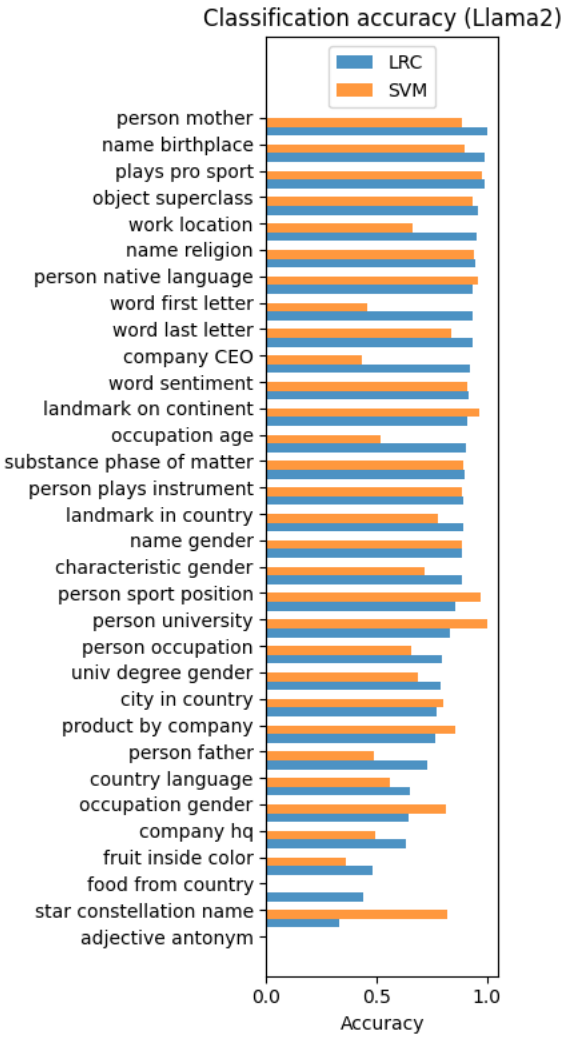


Figure 7: Classification accuracy broken down by relation for LRC (ours) compared to SVM on Llama2-7b. Our method outperforms SVM on most, but not all, relations.

different train / test splits, we calculate significance for each random split separately to avoid double-counting samples which may occur in different splits. This should make our significance estimate more conservative than if we sum the results across all splits.

In order to simplify the significance calculation, the scores are not reweighted by relation as is done in the results in the paper, so if a relation has many more samples than another relation, we do not reweight to account for that in this calculation. As a result, the LRC and SVM scores per iteration are slightly different than appears earlier in the paper. P-value calculations for Llama2-7b are shown in Figure 7, and for GPT-J in Figure 8.

For Llama2-7b, our method is statistically significantly better than SVM for both classification

Classification accuracy (Llama2-7b)				
Seed	Test samples	LRC	SVM	P-val
42	3324	0.842	0.811	9e-4
43	3326	0.845	0.804	1e-5
44	3319	0.839	0.808	9e-4
45	3354	0.838	0.816	0.016
46	3335	0.843	0.803	2e-5

Causality (Llama2-7b)				
Seed	Test samples	LRC	SVM	P-val
42	1527	0.762	0.652	3e-11
43	1533	0.733	0.606	7e-14
44	1517	0.740	0.633	2e-10
45	1497	0.764	0.607	3e-20
46	1497	0.723	0.627	2e-8

Table 7: Statistical significance calculation for classification accuracy comparison for our method (LRC) compared with SVM using Llama2-7b. All comparisons are at subject layer 17. We use object layer 21 for LRC. All P-values from each seed for both classification accuracy and causality are well below the 0.05 threshold for statistical significance. In order to simplify the significance calculation, these scores are not reweighted by relation as is done in the results in the paper, so if a relation has many more samples than another relation, we do not reweight to account for that in this calculation.

Classification accuracy (GPT-J)				
Seed	Test samples	LRC	SVM	P-val
42	2181	0.825	0.793	0.007
43	2129	0.803	0.800	0.818
44	2176	0.784	0.816	0.008
45	2173	0.789	0.791	0.882
46	2236	0.812	0.789	0.0517

Causality (GPT-J)				
Seed	Test samples	LRC	SVM	P-val
42	1049	0.699	0.546	6e-13
43	1054	0.733	0.602	1e-10
44	1088	0.716	0.581	4e-11
45	1014	0.735	0.570	7e-15
46	1097	0.718	0.560	1e-14

Table 8: Statistical significance calculation for classification accuracy comparison for our method (LRC) compared with SVM using GPT-J. All comparisons are at subject layer 14. We use object layer 20 for LRC. The classification accuracy results for LRC are not statistically significant compared with SVM, but the causality results are significantly significant. In order to simplify the significance calculation, these scores are not reweighted by relation as is done in the results in the paper, so if a relation has many more samples than another relation, we do not reweight to account for that in this calculation.

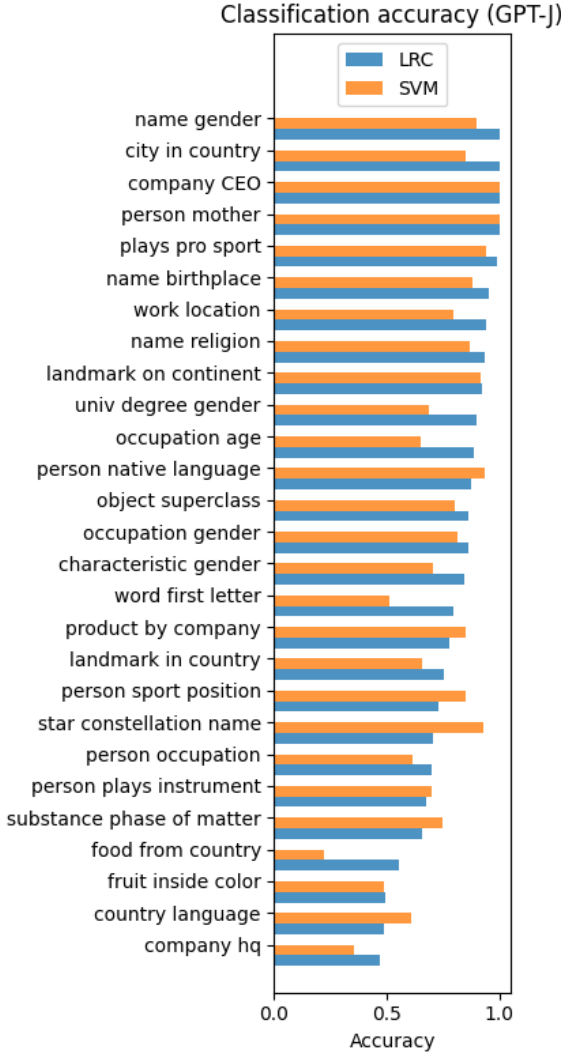


Figure 8: Classification accuracy broken down by relation for LRC (ours) compared to SVM on GPT-J. Our method outperforms SVM on most, but not all, relations.

accuracy and causality. However, for GPT-J, the classification accuracy difference is not statistically significant between our method and SVM, but our method does outperform SVM on causality with statistical significance.

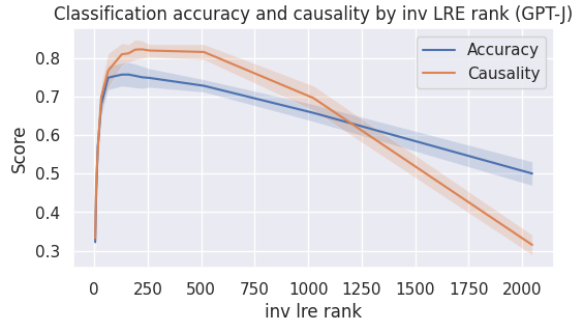


Figure 9: Classification accuracy and causality on the relations dataset by LRE inversion rank on GPT-J. Shaded area indicates standard deviation after five seeds.

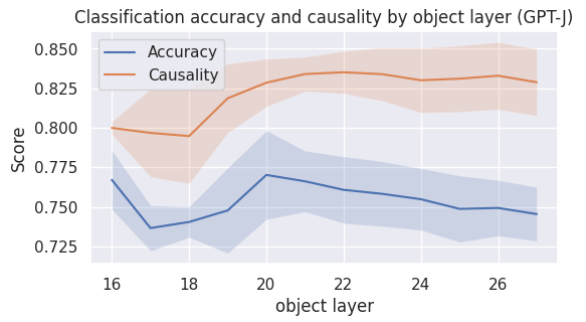


Figure 10: Classification accuracy and causality on the relations dataset by LRE object layer on GPT-J with subject layer 15. Shaded area indicates standard deviation after five seeds.

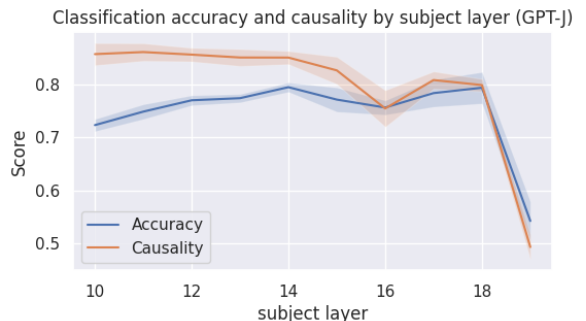


Figure 11: Classification accuracy and causality on the relations dataset by LRE subject layer on GPT-J. Shaded area indicates standard deviation after five seeds.